METEOROLOGICAL APPLICATIONS
Meteorol. Appl. (2013)
Published online in Wiley Online Library
(wileyonlinelibrary.com) DOI: 10.1002/met.1374

Statistical relationship between atmospheric circulation and extreme precipitation in La Plata Basin

Christian R. Garavaglia,[a,c] Moira E. Doyle[a,b]* and Vicente R. Barros[a,b]

[a] *UMI-IFAECI, Centro de Investigaciones del Mar y la Atmósfera (CIMA/CONICET-UBA), Buenos Aires, Argentina*
[b] *Departamento de Ciencias de la Atmósfera y los Océanos, Universidad de Buenos Aires, Argentina*
[c] *Servicio Meteorológico Nacional, Buenos Aires, Argentina*

ABSTRACT: Empirical conditional probabilities of extreme monthly precipitation averaged over three regions of the southern part of the La Plata basin were calculated as a function of three atmospheric indices: two of them represent low level moisture convergence and the third is related to the mid tropospheric circulation over southern South America. The first region includes southern Paraguay, northeastern Argentina, north of Uruguay and the western sector of southern Brazil, the second region stretches over part of southern Brazil, while the third region, surrounding the Plata Estuary extends over western Uruguay and eastern Argentina between 37 ° S and 32 ° S. Regional monthly precipitation was considered extreme when it exceeded its mean value plus one standard deviation. Conditional empirical probabilities of Months with Extreme Precipitation (MEP) are more than twice and even four times higher than climatic probabilities when they are calculated under the restriction that the atmospheric indices were beyond certain extreme thresholds empirically defined. Combined conditional probability is even higher when the values of two or the three indices over their respective thresholds take place at the same time, but these cases are less frequent. The index that renders higher conditional probabilities is the one that accounts for the low level moisture convergence in a region that is basically to the west and outside of the three regions. This reflects the fact that most of the mesoconvective systems, which originate to the west of these regions and then move eastwards, produce heavy precipitation that lead to monthly accumulated extremes. Copyright © 2013 Royal Meteorological Society

KEY WORDS extreme monthly precipitation; probabilities; floods; southeastern South America; indexes; moisture convergence; mid-level tropospheric circulation

Received 22 May 2012; Revised 12 October 2012; Accepted 21 October 2012

1. Introduction

La Plata Basin with over 3 million km^2 is the second largest in South America and the fifth in the world. It stretches over five countries in southeastern South America, encompassing all Paraguay, southern Brazil, south-eastern Bolivia, eastern Argentina and a large part of Uruguay. The population of this basin is approximately 70 million and projections indicate that it will increase steadily, reaching 145 million people by 2025 and therefore likely boosting the exposure of people, infrastructure and services to extreme precipitation and floods.

The Plata Basin includes three large rivers; the Paraná, Paraguay and Uruguay rivers (Figure 1). In the Argentine sector, the Paraguay and Paraná rivers flow over a region characterized by very small terrain slopes and slow superficial runoffs. Severe floods are recurrently caused by rivers overflowing their banks in different sectors of the basin (Coronel *et al*., 2006). These overbank floods are often the consequence of heavy rainfall over the basin upstream in southern Brazil and Paraguay which became more frequent after the 1970s (Camilloni and Barros, 2003; Barros *et al*., 2004).

In addition, very flat lands with slow drainage in central and eastern Argentina are also subject to floods not only from overflows of small rivers and brooks, but because of the stagnation of excess water. Although these floods are the consequence of large local precipitation, they are also modulated by other multiple factors: soil moisture saturation which may be the outcome of intense localized rainfall in a short time period or above normal precipitations over several consecutive months, evaporation and surface runoff that is highly dependent on land cover and topography. These factors made it difficult to find a simple relationship between these floods and local or regional precipitation.

In addition, floods over these flat lands take place at different scales, both in time and space, ranging from a few kilometres to several hundred kilometres and from days to a year or more; the huge ones are not rare and constitute a feature of the hydrology of the southern part of La Plata basin in Argentina (Latrubesse and Brea, 2009). Although a comprehensive statistical and physical analysis of these floods is still lacking, in part due to the limited local information, press reports, satellite information and precipitation data indicate, as shown in Section 3, that the more important floods in size and duration originate from large amounts of accumulated precipitation in the scale of a month or more.

Regarding extreme precipitation, Boulanger *et al*. (2005) worked with a spatially averaged precipitation index over the La Plata basin and found that there has been a significant trend toward stronger precipitation since the mid-1960s, with a marked increase between December and February on the

* Correspondence to: M. Doyle, Dto. Cs. De la Atmósfera y los Océanos, Ciudad Universitaria, Pabellón II, 2do piso, 1428 Buenos Aires, Argentina. E-mail: doyle@cima.fcen.uba.ar

Copyright © 2013 Royal Meteorological Society

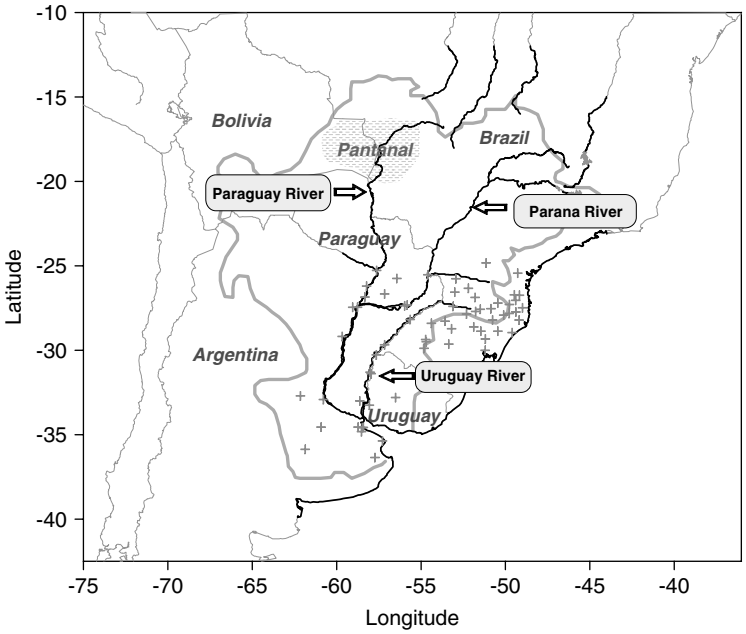

Figure 1. La Plata Basin geographic limits, main rivers, and weather stations used.

border between the humid and semi-arid regions in Argentina. Also, Haylock *et al*. (2006) found positive trends in extreme daily precipitations over Argentina, southern Brazil, Paraguay and Uruguay. Analysing extreme precipitation in the southern part of La Plata basin, Re and Barros (2009) found that since 1960 the number of events with rain above 100 mm in less than 2 days in central and eastern Argentina increased by 50%. Likewise, Penalba and Robledo (2009) found positive trends in the number of rainy days and days with extreme precipitations in that area.

Doyle *et al*. (2012) showed that extremely high rainfall months in southern La Plata basin are related to low level circulation anomalies. Other papers found extreme precipitation connections with upper circulation in the region. For instance precipitation associated with strong jets in South America are considerably more than expect from climatology (Liebmann *et al*., 2004a). Also extreme rainfall in Brazil is associated with the South Atlantic Convergence Zone (SACZ) positive phase which in turn is related to upper wavetrain patterns (Carvalho *et al*., 2004).

Since extreme precipitations play a key role in the occurrence of regional flooding, further understanding of the link between atmospheric circulation and extreme precipitation at monthly timescale is not only of interest *per se*, but also helps understanding the atmospheric conditions that may lead to extended floods over the flat lands of the southern part of the La Plata basin. This understanding is relevant in the context of climate change since climate model projections for the 21st Century indicate increasing annual precipitation over this region, (IPCC, 2007) continuing the detected trends, which started in the 1970s (Barros *et al*., 2000, 2008; Liebmann *et al*., 2004b). These positive trends have already been observed in the precipitation of above normal and extremely high rainfall months (Doyle *et al*., 2012) in recent decades.

The complexity of the atmospheric processes that lead to extreme monthly precipitation in a region can be addressed with different approaches. This paper analyses the probability of occurrence of extreme regional average precipitation over part of La Plata basin as a function of atmospheric indices related to the tropospheric circulation.

2. Data

Monthly precipitation series of the period 1979/2004 were obtained from the Argentine National Weather Service, the Agência Nacional de Águas (ANA) and National Weather Service of Brazil, the National Weather Direction of Uruguay and the Direction of Meteorology and Hydrology of Paraguay. Only those series that have a small percentage of missing data, i.e. less than 10%, were used for the subsequent analysis; they correspond to 64 stations distributed over the southern and eastern La Plata Basin (Figure 1).

Tropospheric variables were taken from the global National Centers for Environmental Prediction – National Center for Atmospheric Research (NCEP–NCAR) reanalysis (Kalnay *et al*., 1996) available on a $2.5 \times 2.5\ ^{\circ}$ latitude–longitude grid. The water vapour transport was calculated using daily specific humidity (q), zonal and meridional wind components (V), and surface pressure. Since most of the water vapour in South America is concentrated, as in many other regions, in the low levels of the troposphere (Berbery and Collini, 2000), the water vapour transport was calculated integrating qV from surface to 700 hPa. Divergence of daily water vapour transport was calculated and then aggregated to obtain monthly values. Monthly average geopotential height at the 500 hPa level was used to characterize mid-level tropospheric circulation.

3. Methodology

Since the precipitation field is highly variable, particularly in the extreme cases, regional averages were used to reduce the variability and to obtain possible relationships with large scale atmospheric conditions. Considering the rainfall regimes in southeastern South America (SESA) as well as the spatial distribution of the available time series, the study area was

Copyright © 2013 Royal Meteorological Society

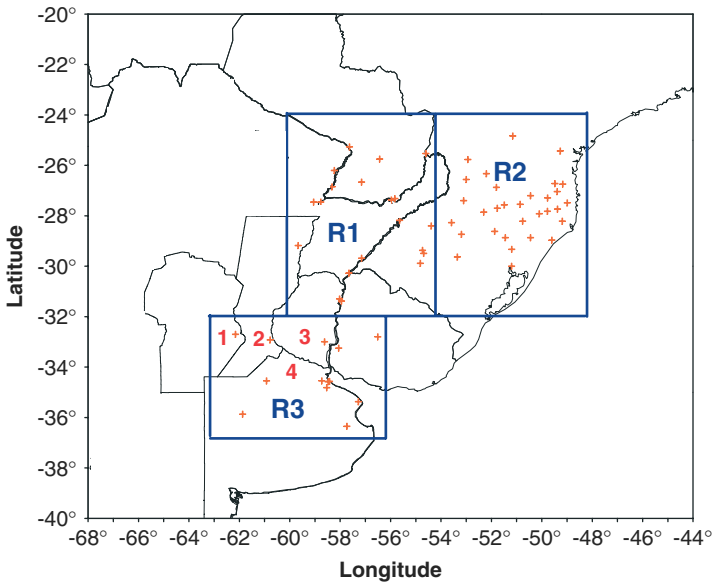

Figure 2. Sub-domains and stations used. Provinces in region R3: (1) Córdoba, (2) Santa Fe, (3) Entre Rios, (4) Buenos Aires. This figure is available in colour online at wileyonlinelibrary.com/journal/met

divided into three regions, R1, R2 and R3, each of them having almost homogeneous precipitation features (Figure 2); areal means of the monthly precipitation in each new area, were then calculated. The first region, R1, extends from 32 ° S to 24 ° S and from 60 ° W to 54 ° W, i.e., this sector includes southern Paraguay, most of northeastern Argentina, north of Uruguay and the western part of southern Brazil. The eastern region, R2, is bounded by 32 ° S and 24 ° S between 54 ° W and 48 ° W and encompasses part of southern Brazil, while the third sub-domain, R3, includes southwestern Uruguay and central-eastern Argentina between 37 ° S and 32 ° S, and 63 ° W and 56 ° W. The number of stations included in each area and used to calculate areal averages are 20 in R1, 31 in R2 and 13 in R3.

The upper tails of the percentiles of monthly regional average precipitation for each of the three regions are presented in Figure 3. Regions R1 and R2 have almost identical percentile distributions, while in the southern region R3, each percentile is associated with a lower rain value. In this study regional monthly precipitation was considered extreme when it exceeded its mean value plus one standard deviation; assuming a normal distribution for the sake of simplicity, they are those exceeding the percentile 83.5, which roughly corresponds to approximately 200 mm in regions 1 and 2 and 137 mm in region 3. In this last region, the most affected by floods over flat lands, this threshold was exceeded in the initial flood month in 9 of 10 of the largest floods while in almost half the events the threshold was also exceeded in the preceding month, Table 1. This threshold may be then considered as an approximate necessary condition for the occurrence of a large flood within that region, but not a sufficient condition because of the number of other factors that influence the occurrence of floods, including the regional spatial distribution of precipitation, which may or may not fall in the more susceptible flooding areas.

Extreme monthly precipitation may be caused either by a combination of atmospheric conditions that may not be extreme or, to the extreme condition of one determinant atmospheric factor. It is likely that since the southern La Plata basin is located in subtropical latitudes, quasi stationary tropospheric troughs may be associated with lasting high regional precipitation. Therefore, to explore this relation the index I500 was defined as:

$$I500_i = \frac{\left\{\left(\overline{\varphi_{1_i}} + \overline{\varphi_{3_i}}\right) - 2.\overline{\varphi_{2_i}}\right\}}{2} \qquad (1)$$

where i denotes month, 1, 2 and 3 correspond to the areas in the latitudinal band between 25 ° S and 45 ° S over the Pacific Ocean (120 ° W to 90 ° W), the South American continent (80 ° W to 60 ° W) and the Atlantic Ocean (50 ° W to 20 ° W) respectively; φ is geopotential height at 500 hPa and the bar indicates area average values. High (low) positive (negative) I500 values are indicative of a predominant trough (ridge) over the continental troposphere.

Doyle *et al*. (2012) showed that extremely high rainfall months in southern La Plata basin were related to low level horizontal moisture convergence, not only over the eastern sector of the basin but over northeastern and central Argentina as well, where most of the mesoconvective systems (MCSs) that affect eastern South America develop. Therefore, monthly means of the divergence of daily water vapour transport integrated between surface and 700 hPa were used to define two new indices, DW and DE, representing moisture convergence west and east of 60 ° W from latitudes 25 ° S to 35 ° S between 65 ° W and 60 ° W in the case of DW and between 60 ° W and 50 ° W for DE.

Extreme precipitation is sometimes the result of complex processes and interactions, that in some cases, though not always, may be determined by extreme atmospheric conditions. These conditions may be represented by indices surpassing a threshold. Since these conditions not always determine extreme precipitation it makes sense to explore the probability of extreme precipitation associated with them. Therefore, based on the three indices here defined, the probability that the regional averaged monthly precipitation reaches extreme values was explored.

The climatic empirical probability of a Month with Extreme Precipitation (MEP) is defined here as the ratio between the number of months with rainfall above the mean plus the standard deviation and the total number of months. As expected according to this definition, the resulting empirical probabilities

Copyright © 2013 Royal Meteorological Society

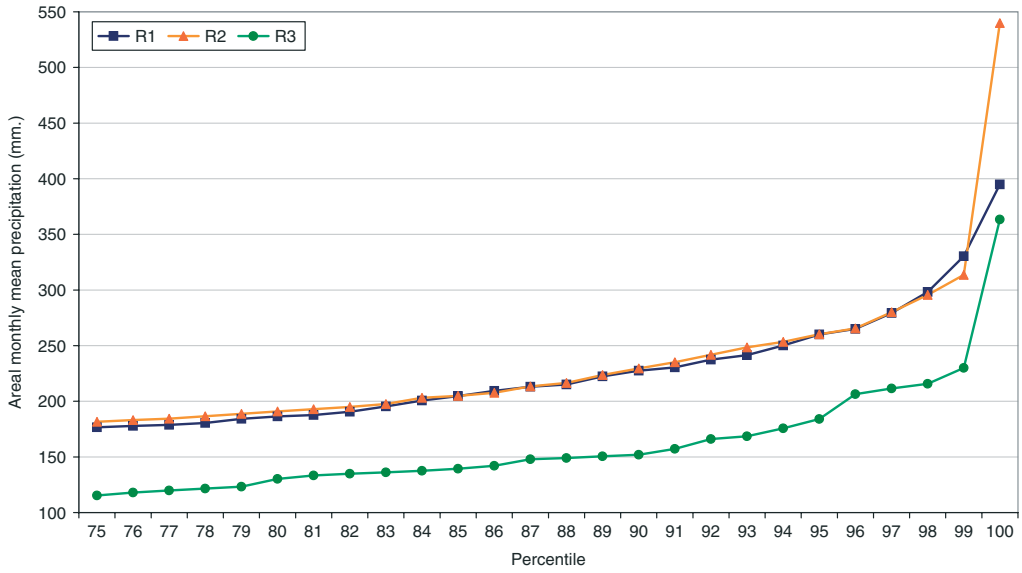

Figure 3. Upper tail of the rainfall percentile distribution in regions R1, R2 and R3. This figure is available in colour online at wileyonlinelibrary.com/journal/met

Table 1. The largest size floods in region R3.

Location	Initial month	Precipitation in the initial month (mm)	Precipitation in the previous month (mm)
Province of Buenos Aires – Salado River basin	April-1980	212.0	138.2
Province of Buenos Aires	November-1985	168.0	165.9
Province of Buenos Aires	March-1987	178.6	149.1
Province of Buenos Aires	March-1988	316.2	70.4
Province of Buenos Aires	March-1992	108.7	71.1
Province of Buenos Aires – Salado River basin	January-1993	147.4	101.2
Provinces of Buenos Aires, Cordoba and Santa Fe	March-1999	163.2	133.7
West of Buenos Aires	October-2000	151.6	78.4
West of Buenos Aires	March-2002	290.7	73.4
North of Buenos Aires and south of Santa Fe and Entre Rios provinces	March-2007	329.4	172.1

Based on LANDSAT satellite information, on the report from the Cámara Argentina de la Construcción 2003 and press reports.

for each region are similar and near 0.17 as can be seen in Table 3.

4. Probabilities of a month with extreme precipitation

4.1. Annual cycle of empiric climatic probabilities

Monthly empiric probabilities of MEP are shown in Figure 4. In each region the annual cycle is characterized by high probabilities during the warm part of the year and low probabilities in winter months (null in R3). Over southern Brazil the most probable months to experience extreme precipitations are January, February and October, while to the south in R3, the transition months October to November and March to April have the highest probabilities.

4.2. Conditional probabilities

To explore atmospheric conditions that enhance the regional probability of occurrence of a MEP, the extreme values of I500, DW and DE indices were calculated and used to estimate empirically the probability of a MEP as a function of them for each region.

Figure 5 shows the number and percent of MEP and months with non-extreme precipitation (MNEP) in regions R1, R2 and R3 for different ranges of indices I500, DW and DE respectively. The empirical climatic probability of MEP is indicated with a full line to discriminate the index values which are associated with higher MEP probability.

One common feature of almost all cases shown in Figure 5 is that the number and the empirical probability of an MEP have either monotonic increase or decrease with the three indices. There is an exception with I500 that shows a decrease of MEP for extreme values in regions 2 and 3. This may be explained because many extreme values of I500 occur during winter time when in general the lack of sufficient moisture inhibits extreme precipitations, as can be seen in Figure 4.

The monotonic feature of MEP empirical probability as a function of the three indices allows defining thresholds of these

Copyright © 2013 Royal Meteorological Society

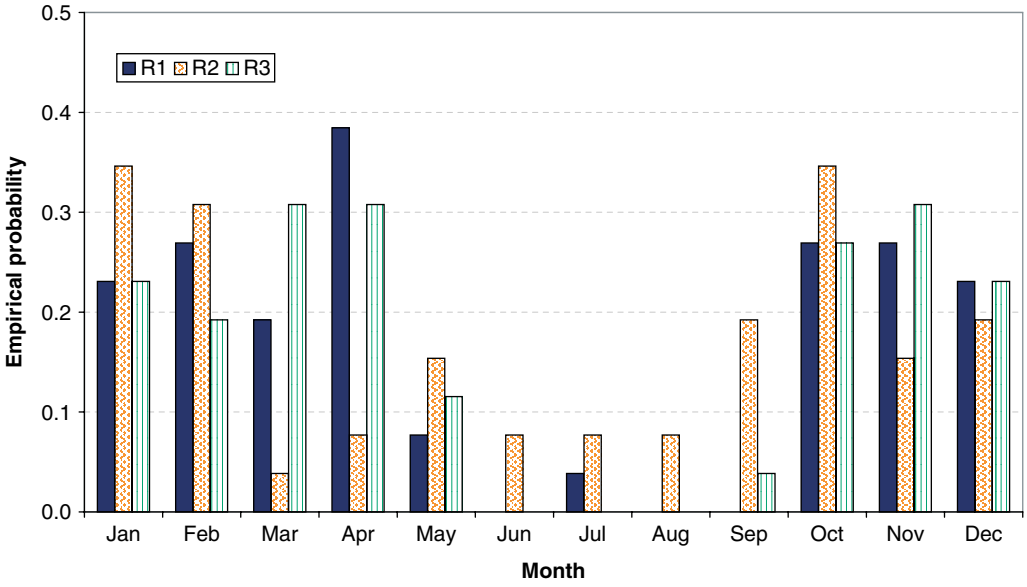

Figure 4. Monthly distribution of empirical probability of a month with extreme precipitation (MEP) for regions R1, R2 and R3. This figure is available in colour online at wileyonlinelibrary.com/journal/met

indices that may increase the probability of an MEP with respect of the empirical one. Of course, the more extreme the value of the index threshold higher will be the probability of an MEP discriminated by this threshold, but on the other hand, fewer cases would be discriminated. Therefore, an arbitrary value of threshold that compromises both, the enhancement of MEP probability and an adequate number of cases, should be selected. Thus, for each index, the thresholds are defined when the probability of MEP is greater than the climatic probability of MEP multiplied by a factor of 1.5 (dashed line in the Figure 5). The advantage of estimating probabilities using thresholds is that it permits to aggregate the cases in blocks with a large enough number of cases to calculate empirical probabilities. Table 2 shows the threshold values selected to find cases with enhanced probability of a MEP for each of the three indices and the three regions. These thresholds are named A1, A2 and A3 corresponding to the I500, DW and DE indices respectively.

The frequency of a MEP is higher under conditions given by high values of I500 as expected, since the presence of a cyclonic circulation entering the continent from the west enhances the probability of occurrence of extreme rainfalls in SESA (Figure 5(a)). However, the threshold selected for R2 (20 gpm) is slightly different from the value assigned to R1 and R3 (10 gpm), indicating that a more intense cyclonic circulation over subtropical South America is required for intense precipitations in the most eastern region of SESA. According to Figure 5(b) and (c) MEPs are more likely to occur under convergence conditions west and/or east of 60 $^{\circ}$ W as indicated by the negative values of DW and DE indices.

Conditional empirical probabilities of MEP in the different regions were calculated according to the thresholds established for each index. The conditional probability based on any of the indices highly increases the probability of a MEP with respect to the climatic probability in all regions (Table 3). However, probabilities in region R1 are remarkable when the DW threshold is considered. Though the probabilities based on threshold indices double in most cases the respective climatic probability, this result is increased almost four times in R1 when extreme convergence dominates west of 60 $^{\circ}$ W. The DW threshold is also important in R2 and R3, even when these regions are farther from the area where DW is calculated; indicating that convergence west of 60 $^{\circ}$ W plays an important role in the extreme precipitation of these regions as well.

To asses to what extent these empirical probabilities of the occurrence of a MEP may result by chance, given the climatic probability of a MEP, a binomial distribution was used:

$$P\ (y \geq k/n)\ (n/k)\ p^k\ (1-p)^{n-k} \qquad (2)$$

where k is the number of observed MEPs in the n months that comply with the selected threshold, p is the climatic probability and y is the success that at least k or more MEPs take place by chance out of the n months. Probabilities lower than 0.05 and 0.01 are indicated in Table 3. Except for R2, where there were only four cases complying simultaneously with the three thresholds, in all other cases the probability that the observed rates were reached by random is very small.

The chosen thresholds of the atmospheric variables make it possible to assess the empirical conditional probability of an extreme monthly precipitation in 144, 78 and 143 months in R1, R2 and R3, respectively. These numbers come from the sum of the months in which the threshold conditions A1, A2 and A3 are attained, minus the coupled common months when threshold conditions A1 and A2, etc. are achieved, plus the common months when A1 and A2 and A3 are simultaneously achieved. That signifies almost half of the months in regions 1 and 3 and a quarter of them in the southern Brazil region. This may indicate that the indices of the atmospheric variables are more appropriated for the Argentine regions and that perhaps a more tailored election for the Brazilian region could render better results.

Selected thresholds also permit elaboration of information on the non occurrence of a MEP. However, it is not the intention to expound here on this aspect, in part because the methodology is similar, but also because the empirical climatic probabilities of no MEP are already large in the three regions and using the cases complying with a threshold increase relatively little these probabilities.

Atmospheric situations where the extreme values of the indices over their thresholds as defined here might occur

Copyright © 2013 Royal Meteorological Society

Table 2. Thresholds for indices I500, DW and DE in regions R1, R2 and R3 for the annual case.

Threshold condition	R1	R2	R3
A1 = I500 >	10 gpm	20 gpm	10 gpm
A2 = DW <	-5×10^{-5} mm s^{-1}	5×10^{-5} mm s^{-1}	-4×10^{-5} mm s^{-1}
A3 = DE <	-1×10^{-5} mm s^{-1}	-3×10^{-5} mm s^{-1}	-2×10^{-5} mm s^{-1}

simultaneously. Therefore, the combined conditional probability of an MEP given that two or all three indices fall within their corresponding threshold tail are also presented in Table 3. In the case when two indices are considered, situations with convergence both west and east of 60 ° W are the most probable ones to cause extreme precipitations in the three regions. However, the probability of a MEP in Region 3 is higher when all three indices fulfill their threshold conditions simultaneously.

4.3. Warm season conditional probabilities

The conditional probabilities calculated in Section 4.2 might be higher than the climatic ones not simply by the influence of atmospheric conditions represented by the circulation indices, but also because these indices have a seasonal variability, which is also present in the frequency of MEPs, as seen in Figure 4. Hence, there is a possibility that higher conditional probabilities with respect to the climatic ones as found previously might be only the result of the seasonal dependence of both MEPs probability and circulation indices. Thus, to rule out this possibility, the former analysis was performed once again but now considering only the calendar months with the highest occurrence of MEPs, namely those of the warm season. This warm season is defined here for each region as the period of consecutive months with high frequency of MEPs based on

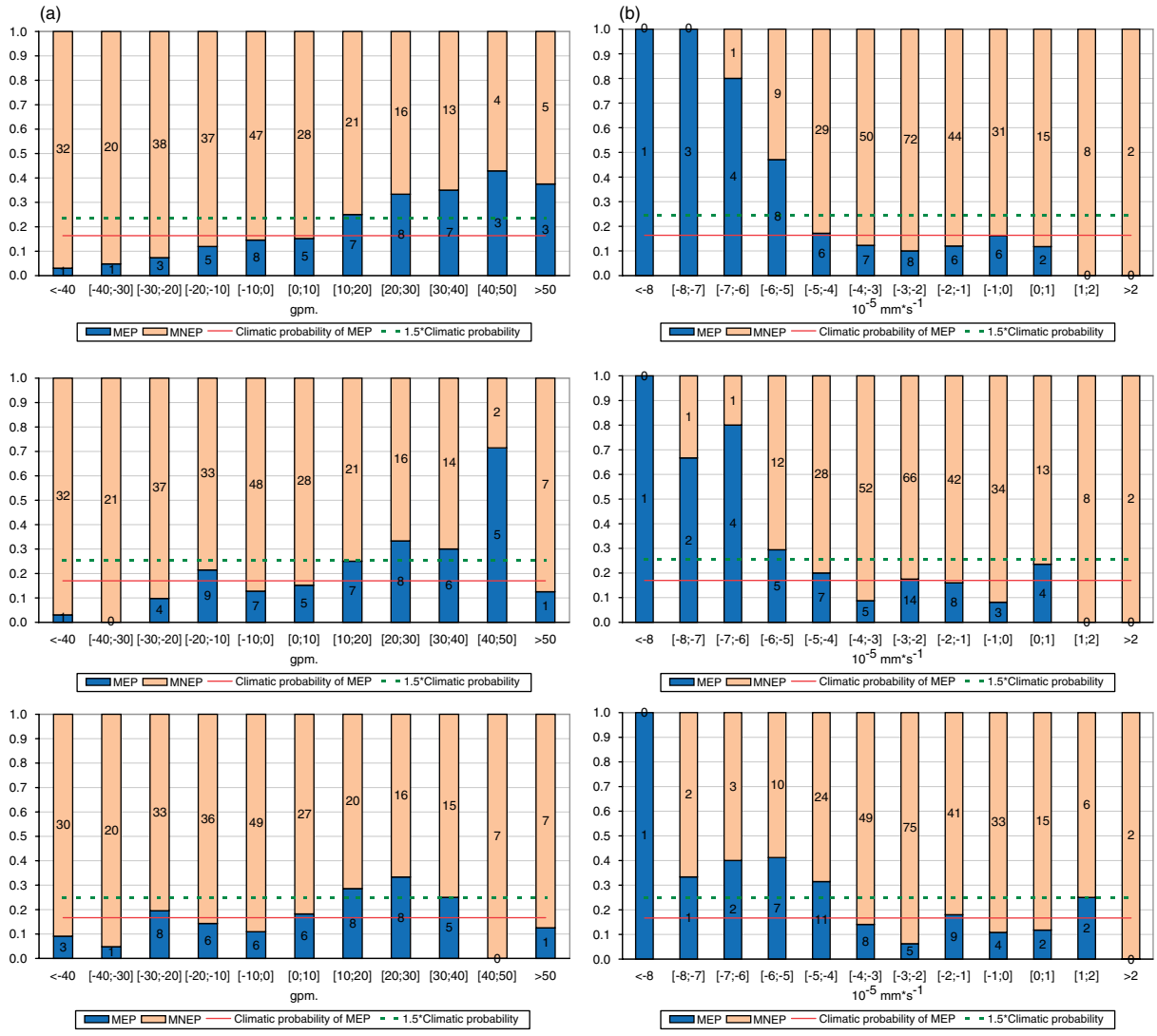

Figure 5. Number of cases of MEP and MNEP as function of index (a) I500, (b) DW, and (c) DE, for R1 (top row), R2 (middle row), and R3 (bottom row) This figure is available in colour online at wileyonlinelibrary.com/journal/met

Copyright © 2013 Royal Meteorological Society

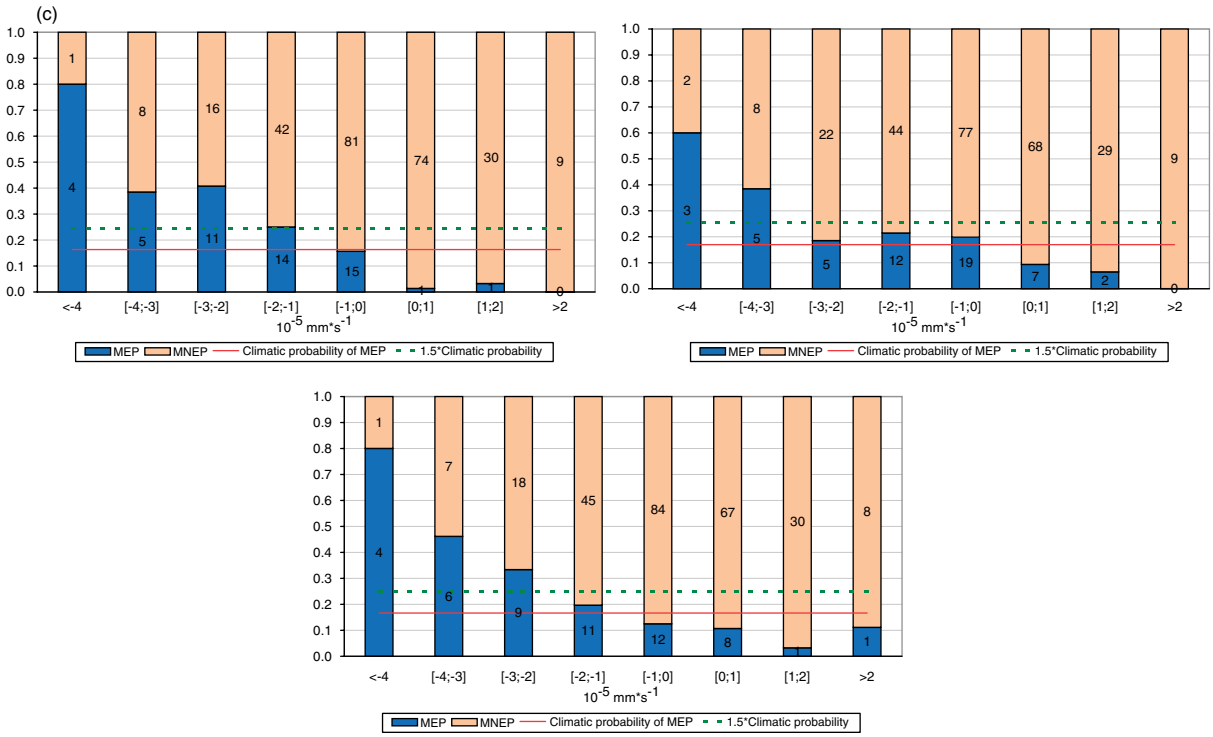

Figure 5. Continued. This figure is available in colour online at wileyonlinelibrary.com/journal/met

Table 3. Empirical probabilities of a MEP.

	R1	R2	R3
Climatic	0.16 (51/312)	0.17 (53/312)	0.17 (52/312)
A1	0.32 (28/87)**	0.34 (20/59)**	0.25 (22/87)**
A2	0.62 (16/26)**	0.46 (12/26)**	0.36 (22/61)**
A3	0.34 (34/101)**	0.44 (8/18)**	0.42 (19/45)**
A1 and A2	0.67 (10/15)**	0.55 (6/11)**	0.39 (13/33)**
A1 and A3	0.40 (20/50)**	0.39 (5/13)*	0.50 (13/26)**
A2 and A3	0.79 (11/14)**	0.60 (3/5)*	0.56 (10/18)**
A1 and A2 and A3	0.78 (7/9)**	0.50 (2/4)	0.57 (8/14)**

The values in brackets show the number of MEPs against the number of months above or below the thresholds indicated in Table 2. * probability of this rate being equal or larger by random is lower than 0.05; ** probability of this rate being equal or larger by random is lower than 0.01.

the annual cycle shown in Figure 4. Consequently, the warm season in regions R1 and R3 goes from October to April, while in region R2 it is slightly more prolonged, starting in September and ending in May.

The definition of the index thresholds follows the same procedure as in the annual case, but the figure analog to Figure 5 is not shown here for the sake of conciseness. Their values are summarized in Table 4. There are no changes in the thresholds for R3, since all MEP events occur during the warm season. Since the other regions present MEP during winter there are some threshold changes with respect to the annual case.

As expected, the empirical climatic probability of a MEP during these warm season periods is higher in all regions than in the annual case, namely 26.4, 20.1 and 26.4% for R1, R2 and R3, respectively, and so are the conditional probabilities associated with the thresholds of the three indices, as described in Table 5.

The chosen indices make it possible to assess the empirical conditional probability of extreme monthly precipitation in only about a third of the warm months, namely in 62, 74, 84 months in R1, R2 and R3, respectively. As in the annual case, probabilities are considerably higher than the climatic value. In R1, with any of the indices the probability raises to more than 0.5, practically doubling the climatic probability. The highest probability is once again given by the use of the DW threshold in R1 as well as in R2 where it is almost four times the climatic probability. In R2, the use of DE and I500 thresholds also enhances probabilities with respect to the climatic case. In R3, the convergence east of 60 ° W results the best index among individual indices, though very similar to DW.

The combined probability including two indices or all three of them once again highly increases the probability of a MEP, but of course these situations are less frequent, especially in the case of the three indices reaching their thresholds. As in the annual case the DW threshold combined with any of the other indices presents the highest probabilities in R1 and R2.

Table 4. As Table 2, but for the warm season as defined in the text.

Condition for threshold	R1	R2	R3
A1 = I500 >	20 gpm	10 gpm	10 gpm
A2 = DW <	-5×10^{-5} mm s^{-1}	-6×10^{-5} mm s^{-1}	-4×10^{-5} mm s^{-1}
A3 = DE <	-2×10^{-5} mm s^{-1}	-3×10^{-5} mm s^{-1}	-2×10^{-5} mm s^{-1}

Copyright © 2013 Royal Meteorological Society

Table 5. As Table 3, but for the warm season as defined in the text.

	R1	R2	R3
Empirical climatic	0.26 (48/182)	0.20 (47/234)**	0.26 (48/182)**
A1	0.57 (20/35)**	0.35 (23/66)**	0.42 (22/53)**
A2	0.70 (16/23)**	0.78 (7/9)**	0.50 (21/42)**
A3	0.51 (18/35)**	0.44 (8/18)*	0.51 (18/35)**
A1 and A2	0.80 (8/10)**	0.83 (5/6)**	0.59 (13/22)**
A1 and A3	0.53 (9/17)*	0.39 (5/13)	0.65 (13/20)**
A2 and A3	0.80 (8/10)**	1.00 (1/1)	0.63 (10/16)**
A1 and A2 and A3	0.83 (5/6)**	1.00 (1/1)	0.67 (8/12)**

* 95% significance; ** 99% significance.

Nonetheless, it is the combination of the three which results in the highest probabilities in all regions except in R2, where the calculated probability should not be considered representative since it was based on only one event.

Since conditional probabilities considering individual or combined thresholds during the warm season are higher than those found in the annual case and moreover, as in the annual case, the conditional probabilities are considerably higher than the climatic ones, it can be concluded that the main driver of the conditional probabilities is the atmospheric circulation as represented by the three indices and not the seasonality of the MEPs.

5. Concluding remarks

The very flat lands of region 3 include areas of very low runoff that are subject to floods when bearing excess water. This excess is determined not only by rainfall at the initial time of the flood, but by other factors that make difficult to find a direct relationship with local or regional rainfall. Nonetheless, in most of the larger floods in R3, a mean regional precipitation exceeding the mean plus one standard deviation was observed on the month that flood starts, Table 1 and Figure 3. This threshold may, in consequence, be regarded as an approximate necessary condition for such floods to start, but not sufficient, as many other factors may be involved in the development of these floods. Therefore, this threshold was used to characterize an MEP event in R3, and consistently in the other two regions.

The empirical climatic probability of an MEP has a well marked annual cycle in the three regions of the south of the La Plata Basin with higher values during the warm part of the year (October to April) and low or null probabilities in winter months (Figure 4). This result is not surprising because of the higher water content of the atmosphere during the warmer months. However, in the southernmost region, the maximum probability is in the transition months of October to November to December and March to April, very much lined up with the annual cycle of precipitation.

Three atmospheric circulation indices *a priori* associated with regional precipitation were calculated to elaborate thresholds related to MEP. One of them represents the monthly average position and intensity of a mid troposphere wave over South America whose extreme values over the threshold are proper of a stationary trough over the west of southern South America. The other two are regional averages of the moisture convergence to the east and west of 60 $^\circ$ W.

Conditional empirical probabilities of an MEP when the given thresholds of the atmospheric variables were attained ranged from 0.25 to 0.62, varying according to the region and the atmospheric variable, but in general were more than twice and even four times higher than climatic empirical probabilities, Table 3. Combined conditional probabilities can be calculated when values of two or three indices attaining their respective thresholds occur simultaneously; they are even higher, ranging from 0.39 to 0.78, but of course they only applied to fewer cases.

Typical tropospheric circulation and low level transport and moisture convergence associated with the highest probability of MEP occurrence are illustrated in Figure 6 which presents the composite of April 1990, October 1997, and March, April and October 2002. These months correspond to the case of the three indices simultaneously attaining their respective threshold with the highest significant conditional probability of MEP in all regions and cases, namely 0.83 (Tables 3 and 5).

In Figure 6(a), the circulation depicts a maximum cyclonic anomaly, centred at 40–45 $^\circ$ S west of the Chilean coast which favours the advection of cyclonic vorticity over SESA. Figure 6(b) shows the generalized water vapour transport coming from the tropical forests with two axis of moisture convergence over regions DW and DE as discussed by Doyle *et al*. (2012), being the western nucleus the most important. This is consistent with the fact that the A2 (threshold of DW) is associated with most of the highest significant conditional probabilities (Tables 3 and 5).

It is worth highlighting that the DW index of monthly moist convergence in central and west Argentina was calculated in an area that does not overlap with the three regions studied here, except with a small part of region 3. The reason for this, at first sight peculiar selection, is that most of the mesoscale convective systems (MCSs) that affect the southern part of La Plata Basin originate west of 60 $^\circ$ W on the eastern slopes of the mountain chains that run parallel at the east of the Andes (Doyle *et al*., 2012) and then move eastwards (Salio *et al*., 2007); the birth and development of these MCSs are favoured by intense moisture transport from the tropics to the subtropics, sometimes with the presence of a low level jet (Nicolini *et al*., 2002). These MCSs produce heavy rainfalls accounting for about 60% of the annual precipitation of the region (Nesbitt *et al*., 2006). Therefore, a quantitative relationship between monthly average of moist convergence to the west of 60 $^\circ$ W and monthly extreme precipitation to the east of that longitude should be expected. In fact, the conditional probabilities of an MEP resulting from moist convergence below the DW index threshold alone or combined with the other indices are almost in all cases the highest in the three regions.

Future scenarios of precipitation features in the Plata Basin are of particular interest in view of the important positive trends during the last decades (Barros *et al*., 2000, 2008; Liebmann *et al*., 2004b). These positive trends were also observed on the extremes of monthly precipitation (Doyle *et al*., 2012). However, the skill of global climate models (GCM) to simulate the climatology of precipitation over La Plata basin is very limited (e.g. Vera and Silvestri, 2009; Saurral, 2010). In general, they underestimate annual precipitation and in some cases do not even properly describe the annual cycle (Saurral, 2010). This is a limitation to exploring future climate scenarios through the direct use of MCGs. One alternative is to use variables well simulated by the MCGs that are related to precipitation. In general, MCGs represent well the large scale atmospheric conditions over South America and neighbouring oceans. When these atmospheric conditions are then related to large scale precipitation features in the observed climate, these relationships can be used in the MCG outputs to simulate future

Copyright © 2013 Royal Meteorological Society

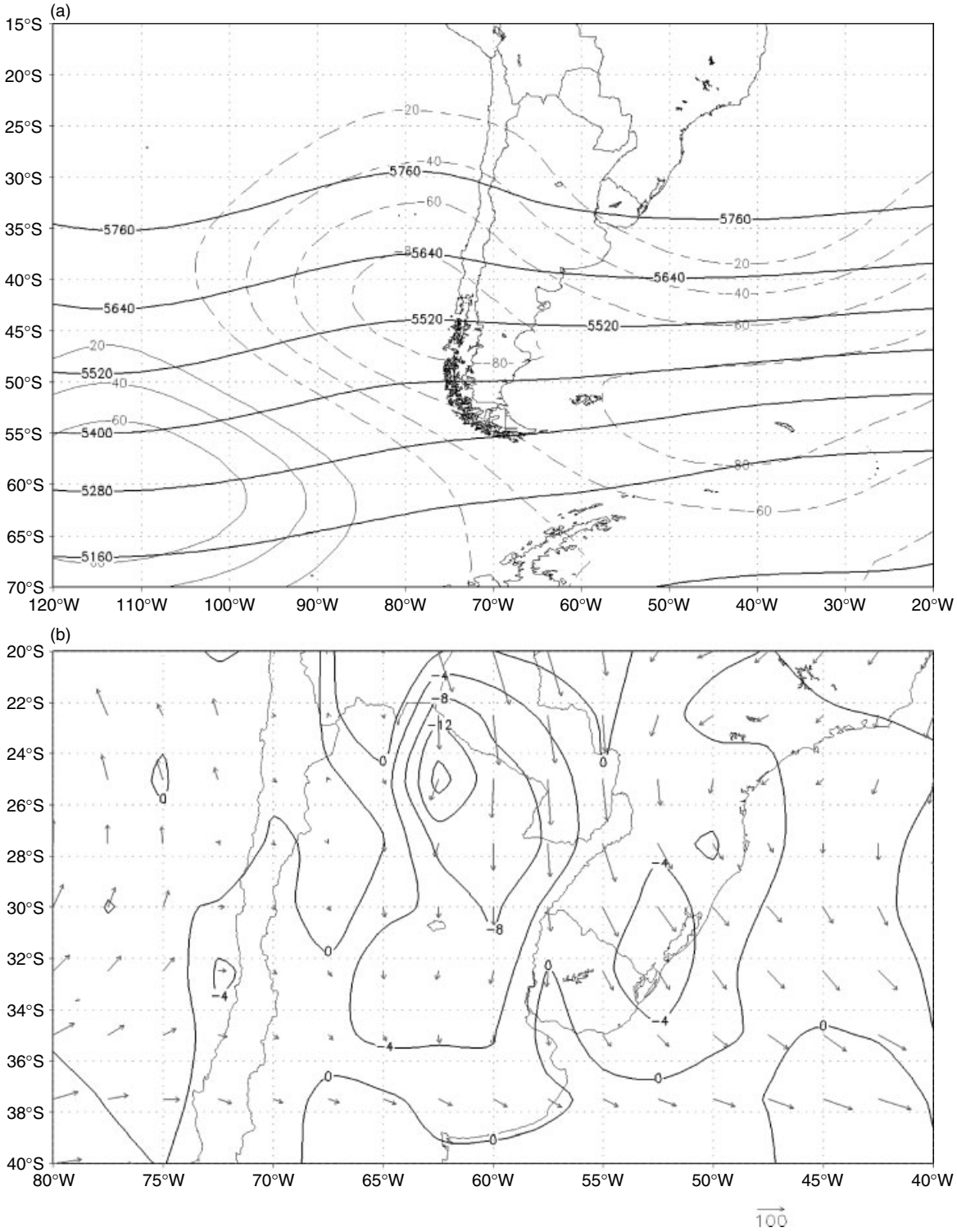

Figure 6. Composite for April 1990, October 1997 and March, April and October 2002 of: (a) Geopotential height (black) at 500 hPa and its anomaly (grey) (gpm) and (b) Low-level water vapour transport (mm m s^{-1}) and convergence (in 10^{-5} mm s^{-1}).

precipitation features, including extreme monthly precipitation probabilities such as the ones studied here.

Acknowledgements

The research leading to these results has received funding from the European Community's Seventh Framework Programme (FP7/2007-2013) under Grant Agreement No. 212492.

References

Barros VR, Castañeda ME, Doyle ME. 2000. Recent precipitation trends in Southern South America East of the Andes: an indication of climatic variability. In *Southern Hemisphere Paleo- and Neoclimates. Key Sites, Methods, Data and Models*, Smolka PP, Volkheimer V (eds). Springer: Berlin; 187–206.

Barros VR, Chamorro L, Coronel G, Báez J. 2004. The major discharge events in the Paraguay River: magnitudes, source regions and climate forcings. *J. Hydrometeorol.* **5**: 1061–1070.

Copyright © 2013 Royal Meteorological Society

Barros VR, Doyle ME, Camilloni I. 2008. Precipitation trends in southeastern South America: relationship with ENSO phases and the low-level circulation. *Theor. App. Climatol.* **93**: 19–33.

Berbery EH, Collini E. 2000. Springtime precipitation and water vapor flux over Southeastern South America. *Mon. Weather. Rev.* **128**: 1328–1349.

Boulanger J-P, Leloup J, Penalba O, Rusticucci M, Lafon F, Vargas W. 2005. Observed precipitation in the Paraná-Plata hydrological basin: long-term trends, extreme conditions and ENSO teleconnections. *Clim. Dyn.* **24**: 393–413.

Cámara Argentina de la Construcción. 2003. El cambio climático y sus consecuencias territoriales. (Climate change and its field consequences). *51st Annual Meeting*, Buenos Aires, Argentina.

Camilloni I, Barros VR. 2003. Extreme discharge events in the Paraná River and their climate forcing. *J. Hydrol.* **278**: 94–106.

Carvalho LMV, Jones C, Liebmann B. 2004. The South Atlantic Convergence Zone: intensity, form, persistence, and relationships with intraseasonal to interannual activity and extreme rainfall. *J. Clim.* **17**: 88–108.

Coronel G, Menéndez A, Chamorro L. 2006. Physiography and hydrology. In *Climate Change in the Plata Basin*, Barros V, Clarke R, Silva Dias P (eds). CIMA-CONICET: Buenos Aires; 44–59.

Doyle ME, Saurral R, Barros VR. 2012. Trends in the distributions of aggregated monthly precipitation over the Plata Basin. *Int. J. Climatol.* **32**: 2149–2162.

Haylock MR, Peterson T, Abreu de Sousa JR, Alves LM, Ambrizzi T, Anunciação YMT, Baez J, Barbosa de Brito JI, Barros VR, Berlato MA, Bidegain M, Coronel G, Corradi V, Garcia VJ, Grimm AM, Jaildo dos Anjos R, Karoly D, Marengo JA, Marino MB, Meira PR, Miranda GC, Molion L, Moncunill DF, Nechet D, Ontaneda G, Quintana J, Ramirez E, Rebello E, Rusticucci M, Santos JL, Trebejo I, Vincent L. 2006. Trends in total and extreme South American temperature 1960–2000 and links with sea surface temperature. *J. Clim.* **19**: 1490–1512.

IPCC. 2007. *Contribution of Working Group I to the Fourth Assessment Report of the Intergovernmental Panel on Climate Change*, Solomon S, Qin D, Manning M, Chen Z, Marquis M, Averyt KB, Tignor M, Miller HL (eds). Cambridge University Press: Cambridge, and New York, NY.

Kalnay E, Kanamitsu M, Kistler R, Collins W, Deaven D, Gandin L, Iredell M, Sha S, White G, Woollen J, Zhu Y, Chelliah M, Ebisuzaki W, Higgins W, Janowiak J, Mo KC, Ropelewski C, Wang J, Leetmaa A, Reynolds R, Jenne R, Joseph D. 1996. The NCEP/NCAR 40-year reanalysis project. *Bull. Am. Meteorol. Soc.* **77**: 437–471.

Latrubesse EM, Brea D. 2009. Chapter 16. Floods in Argentina. *Dev. Earth Surf. Processes* **13**: 333–349.

Liebmann B, Kiladis G, Vera C, Saulo C, Carvalho L. 2004a. Subseasonal variations of rainfall in South America in the vicinity of the low-level jet east of the Andes and comparison to those in the South Atlantic Convergence Zone. *J. Clim.* **17**: 3829–3842.

Liebmann B, Vera C, Carvalho L, Camilloni I, Barros V, Hoerling M, Allured DA. 2004b. An observed trend in central South American precipitation. *J. Clim.* **17**: 4357–4367.

Nesbitt SW, Cifelli R, Rutledge SA. 2006. Storm morphology and rainfall characteristics of TRMM precipitation features. *Mon. Weather. Rev.* **134**: 2702–2721.

Nicolini M, Saulo C, Torres JC, Salio P. 2002. Strong South American low-level jet events characterization during warm season and implications for enhanced precipitation. *Meteorológica* (Special Issue on South American Monsoon System) **27**: 59–69.

Penalba OC, Robledo FA. 2009. Spatial and temporal variability of the frequency of extreme daily rainfall regime in the La Plata Basin during the 20th century. *Clim. Change.* **98**: 531–550.

Re M, Barros V. 2009. Extreme rainfalls in SE South America, 2009. *Clim. Change.* **96**: 119–136.

Salio PV, Nicolini M, Zipser EJ. 2007. Mesoscale convective systems over southeastern South America and their relationship with the South American Low-Level Jet. *Mon. Weather. Rev.* **135**: 1290–1309.

Saurral R. 2010. The hydrologic cycle of the La Plata Basin in the WCRP-CMIP3 multi-model dataset. *J. Hydrometeorol.* **5**: 1083–1102.

Vera CS, Silvestri G. 2009. Precipitation interannual variability in South America from the WCRP-CMIP3 multi-model dataset. *Clim. Dyn.* **32**: 1003–1014.

Copyright © 2013 Royal Meteorological Society